

Low-latency Event-based Object Detection with Spatially-Sparse Linear Attention

Haiqing Hao¹ Zhipeng Sui¹ Rong Zou² Zijia Dai³ Nikola Zubić²
Davide Scaramuzza² Wenhui Wang¹

¹Tsinghua University ²Robot and Perception Group, University of Zurich ³ShanghaiTech University

Abstract

Event cameras provide sequential visual data with spatial sparsity and high temporal resolution, making them attractive for low-latency object detection. Existing asynchronous event-based neural networks realize this low-latency advantage by updating predictions event-by-event, but still suffer from two bottlenecks: recurrent architectures are difficult to train efficiently on long sequences, and improving accuracy often increases per-event computation and latency. Linear attention is appealing in this setting because it supports parallel training and recurrent inference. However, standard linear attention updates a global state for every event, yielding a poor accuracy-efficiency trade-off, which is problematic for object detection, where fine-grained representations and thus states are preferred. The key challenge is therefore to introduce sparse state activation that exploits event sparsity while preserving efficient parallel training. We propose Spatially-Sparse Linear Attention (SSLA), which introduces a mixture-of-spaces state decomposition and a scatter-compute-gather training procedure, enabling state-level sparsity as well as training parallelism. Built on SSLA, we develop an end-to-end asynchronous linear attention model, SSLA-Det, for event-based object detection. On Gen1 and N-Caltech101, SSLA-Det achieves state-of-the-art accuracy among asynchronous methods, reaching 0.375 mAP and 0.515 mAP, respectively, while reducing per-event computation by more than 20× compared to the strongest prior asynchronous baseline, demonstrating the potential of linear attention for low-latency event-based vision.

1. Introduction

Event cameras provide sequential visual data with spatial sparsity and high temporal resolution, lending great promise for low-latency perception [9, 11, 29]. Normally, asynchronous event-based neural networks realize this low-latency advantage by asynchronously updating their predic-

tions every time a new event arrives [36, 37]. This event-driven strategy makes event cameras particularly appealing for object detection in critical, latency-sensitive scenarios, such as automotive driving [11], drone obstacle avoidance [7], and vision-based control [16].

Despite much lower latency, existing asynchronous event-based neural networks lag behind their synchronous counterparts in accuracy [32, 49]. The reason stems from two coupled architectural bottlenecks of the asynchronous model. One is the parallel-recurrent bottleneck: the event-by-event inference paradigm naturally relies on recurrent architectures, whereas efficient training on long sequential events requires parallelization along the sequence dimension [14, 39]. The other is the accuracy-efficiency trade-off: improving accuracy normally requires larger and deeper models, while scaling the model increases per-event computation and consequently latency. A natural solution for this trade-off is to exploit the sparsity of events for sparse activation [36, 37]. Nevertheless, as the receptive fields expand layer-by-layer in deep networks, even sparse inputs would lead to dense activations. To preserve sparsity in deep layers, efforts have been made in designing specific architectures, but the accuracy [11] improvement was limited.

Recently, linear attention¹ has been introduced as a promising asynchronous event-based model architecture since it naturally solves the parallel-recurrent bottleneck [13, 20, 31, 46, 47]. However, existing methods have been limited to relatively simple global-level classification tasks [38, 41], while more challenging local-level tasks, like object detection, remain unexplored. The obstacle lies in the poor accuracy-efficiency trade-off, due to the lack of state-level sparsity, *i.e.*, linear attention updates all elements of its state, making per-event computation scale with the state size. This is problematic for object detection, in which fine-grained spatial representation and therefore a large state size is preferred [14]. It can be straightforward to sparsify the state activation, but the key challenge lies in maintaining

¹For convenience, here we use linear attention as a shorthand for parallel-trainable linear recurrent models, including state space models (SSMs) and linear recurrent neural networks (linear RNNs).

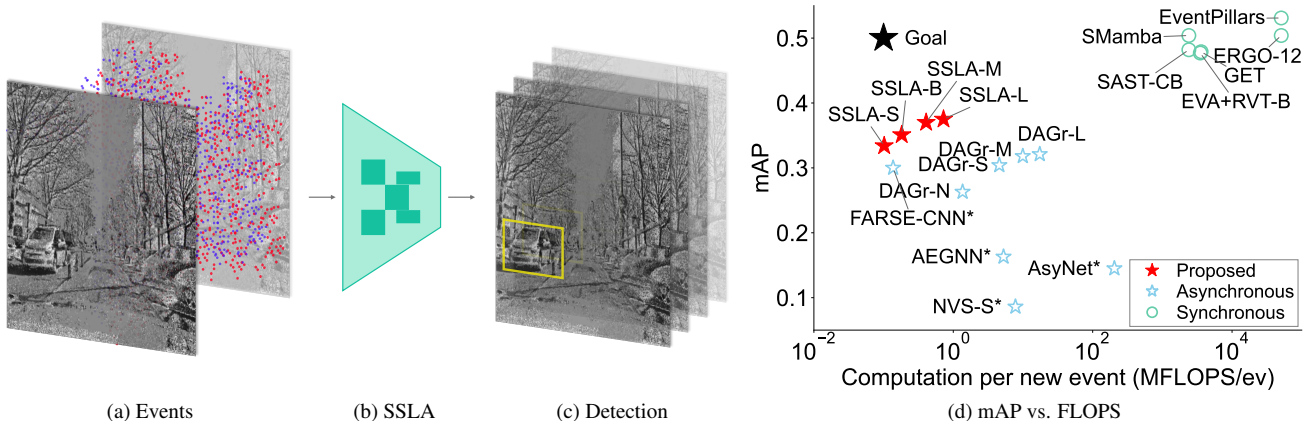


Figure 1. Our method processes (a) asynchronous event sequence with (b) a sparsely activated linear attention neural network for (c) low-latency event-based object detection. On the Gen1 dataset, our SSLA-Det models achieve SoTA asynchronous mAP and lower FLOPS compared with previous asynchronous baselines (d). * refers to AP₅₀.

the parallel training while gaining the sparsity.

We address this challenge by introducing Spatially-Sparse Linear Attention (SSLA), a linear attention module with state-level sparsity while preserving its parallel training advantages. To enable state-level sparsity, we introduce a *mixture-of-spaces* (MOS) structure inspired by [6] that decomposes the global state into sub-states with spatial overlapping receptive fields, and each event activates only a few sub-states based on its location. To preserve the sparsity in deep networks, we aggregate the activations of each event from all its activated sub-states, preventing the expansion of the activated region. We further propose a *position-aware projection* (PAP) that projects events based on their relative position within every activated sub-state, injecting state-relative spatial priors. We derive a *scatter-compute-gather* training procedure that parallelizes this sparse activation structure by sequence-level reorganization. Specifically, events are scattered into state-specific subsequences, computed in parallel by linear attention, and then gathered back into the original event sequence. In this way, SSLA makes linear attention sparse in space, recurrent in time, and parallel in training.

Built on the SSLA module, we present SSLA-Det, to the best of our knowledge, the first asynchronous linear attention model for low-latency event-based object detection (Fig. 1 (a)-(c)). Experiments on Gen1 and N-Caltech101 show that SSLA-Det achieves a substantially improved accuracy-efficiency trade-off over prior asynchronous methods (Fig. 1 (d)), including state-of-the-art (SOTA) asynchronous mAP (0.375 on Gen1 and 0.515 on N-Caltech101) at much lower computational cost ($> 20\times$ reduction compared with previous SOTA [11]). Our contributions are as follows:

- We propose an SSLA module for sequential event mod-

eling, including a MOS structure for state-level sparsity, PAP for spatial prior encoding, and a scatter-compute-gather procedure for efficient parallel training.

- We present SSLA-Det, to the best of our knowledge, the first end-to-end asynchronous linear attention model for event-based object detection.
- SSLA-Det reaches a new accuracy-efficiency frontier, reaching 0.375 mAP on Gen1 and 0.515 mAP on N-Caltech101, with substantially lower computation ($> 20\times$ reduction) than prior asynchronous SOTA.

2. Related Work

2.1. Asynchronous Event-based Neural Networks

Asynchronous event-based neural networks treat event camera data as different geometric structures to leverage their spatial sparsity. This strategy includes graphs [3, 4, 11, 22, 37], submanifolds [25, 36], point clouds [39, 43], and sequences [14, 19, 38, 41]. Graph-based methods [2-4, 11, 22, 37] transform events into sparsely connected spatial-temporal graphs, and derive local update rules on the graph for recurrent inference. However, they have limitations in temporal accumulation [4], failing to handle long event sequences. Submanifold methods [25, 36] assume that events lie on a spatial submanifold, and conduct convolution only on the submanifold to keep sparsity. However, this submanifold assumption does not strictly hold, and thus leads to suboptimal performance. Point cloud methods [9, 43] represent events as spatial-temporal 3-D point clouds, and process with PointNet [35]. This approach is limited to shallow neural networks, and thus has difficulty in challenging tasks. Sequence-based methods use causal sequence-to-sequence models for event processing including softmax attention or linear recurrent models. For ex-

ample, [19] uses attention to process batched events at each timestep. EventSSM [38] and S7 [41] use SSMs, which enable parallel training and recurrent inference, but are limited to global-level classification tasks. EVA [14] explores linear attention for event-based object detection but still demands a dense backbone, while our method is fully end-to-end asynchronous.

2.2. State-level Sparsity in Linear Attention

A recent direction to improve linear attention is to introduce state-level sparsity. Mixture-of-Memories [6] and Sparse State Expansion [28] maintain multiple independent states and use a learned router to send each token to only a few memories. Our SSLA follows the same sparse state activation idea but targets event-based vision and exploits spatial structure. Instead of learning-based routing, we scatter events according to their locations, yielding spatially-sparse state updates suitable for event-based vision. Concurrent work [40] also introduces local states in linear attention for local-level event-based vision, but requires spatial contraction at discrete timestamps, which is not asynchronously, event-by-event trainable. Our work, instead, uses a scatter-compute-gather algorithm to reorganize events to subsequences and does not rely on spatial contraction, which is fully event-by-event asynchronous.

3. Method

3.1. Problem Formulation.

Event camera data are represented as a sequence of events $\mathcal{E} = \{e_i\}_{i=1}^L$, where each event $e_i = (\mathbf{x}_i, t_i, p_i)$ carries its spatial coordinates $\mathbf{x}_i \in \mathbb{R}^2$, a timestamp $t_i \in \mathbb{R}$ and a polarity $p_i \in \{+1, -1\}$. The sequence is temporally ordered so that $t_i \leq t_{i+1}$. Asynchronous event processing learns a causal stateful neural network \mathcal{M} that takes \mathcal{E} as input and makes predictions incrementally, which could be formulated as a causal sequence-to-sequence problem from $\{e_i\}_{i=1}^L$ to $\{\hat{y}_i\}_{i=1}^L$. Specifically, for each new incoming event e_i , the model updates its state \mathbf{S}_i and produces a new prediction \hat{y}_i , as $(\hat{y}_i, \mathbf{S}_i) = \mathcal{M}(e_i, \mathbf{S}_{i-1})$.

3.2. Preliminaries: Linear Attention

Linear attention models (linear RNNs, SSMs) are linear-time alternatives to softmax attention [44] for sequence-to-sequence modeling. Causal linear attention has an equivalent parallel and recurrent form, which enables both parallel training and recurrent inference [20]. Given an input sequence of embeddings $\{\mathbf{z}_i\}_{i=1}^L$, a causal linear attention module updates its hidden state \mathbf{S}_i and computes outputs $\{\mathbf{o}_i\}_{i=1}^L$ as

$$\begin{aligned} \mathbf{S}_i &= g(\mathbf{z}_i) \odot \mathbf{S}_{i-1} + \phi(\mathbf{z}_i), \\ \mathbf{o}_i &= \rho(\mathbf{z}_i, \mathbf{S}_i), \end{aligned} \quad (1)$$

where g, ϕ, ρ are learnable projections (gating, updating, and output) and \odot is the Hadamard product. This recurrent linear attention is parallel trainable with parallel scan [13] or chunk-wise algorithms [46], which is training-efficient on long event sequences. For convenience, we denote the map of linear attention as **LinearAttention** : $\{\mathbf{z}_i\}_{i=1}^L \mapsto \{\mathbf{o}_i\}_{i=1}^L$ in this paper.

3.3. Spatially-Sparse Linear Attention

We introduce the Spatially-Sparse Linear Attention (SSLA) module for asynchronous event processing, which is illustrated in Fig. 2. SSLA module takes an event sequence \mathcal{E} with embeddings $\mathbf{v}_i \in \mathbb{R}^{D_{in}}$ as input, and outputs \mathcal{E} with updated embeddings $\mathbf{o}_i \in \mathbb{R}^{D_{out}}$. To exploit the spatial sparsity of events, we first introduce a *mixture-of-spaces* (MOS) decomposition of the hidden state, which enables state-level spatial sparsity. We incorporate a *position-aware projection* (PAP) in the SSLA module to encode spatial priors to event embeddings. To preserve the training efficiency of linear attention, we derive a *scatter-compute-gather* procedure for parallel training by reorganizing events to independent subsequences.

3.3.1. Sparse State Activation with Mixture-of-Spaces

We define Ω as the spatial domain where \mathcal{E} lies, and decompose it into spatially local patches, with each patch maintaining its own state. We construct these patches by applying a sliding window of size $P \times P$ with a stride of 1 over Ω . Let $\mathcal{P} = \{1, \dots, K\}$ denote the indices of these patches, where each patch $k \in \mathcal{P}$ covering a spatial region $\mathcal{R}_k \subset \Omega$ maintains state \mathbf{S}_k .

For e_i at \mathbf{x}_i , we activate only specific patches that contain \mathbf{x}_i for sparse state activation. We define the set of active patches of e_i as

$$\mathcal{K}_i = \{k \in \mathcal{P} \mid \mathbf{x}_i \in \mathcal{R}_k\}. \quad (2)$$

We pad the image domain to ensure that each event activates a constant number of states, *i.e.*, $|\mathcal{K}_i| = P^2 \triangleq A$. These A states are updated by Eq. (1) with event embeddings, and generate interim outputs $\{\mathbf{o}_{i,k}, k \in \mathcal{K}_i\}$. All active patches share the same linear attention parameters but maintain independent states. We aggregate the interim outputs as the updated embedding from all activated patches:

$$\mathbf{o}_i = \sum_{k \in \mathcal{K}_i} \mathbf{o}_{i,k}, \quad (3)$$

After aggregation, the embedding sequence length is unchanged, which preserves sparsity in deep layers.

3.3.2. Position-Aware Projection

Sharing identical embeddings \mathbf{v}_i for one event in all its activated patches ignores the spatial prior of the event, since the event is located at different and relative positions in

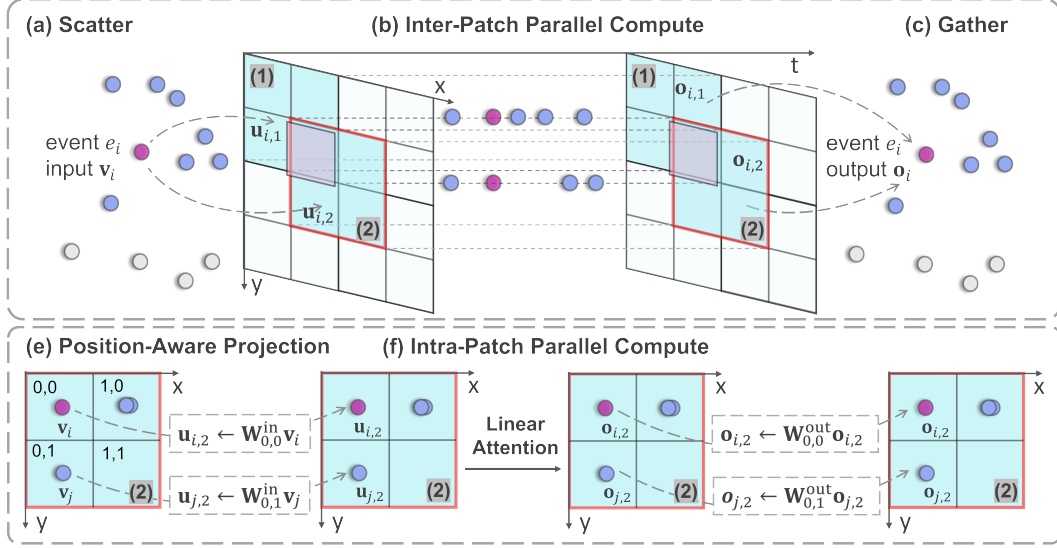


Figure 2. **Overview of the Spatially-Sparse Linear Attention (SSLA) Module.** (1) and (2) are 2×2 sliding window patch examples on the spatial domain. Each event is (a) scattered into multiple patches that spatially cover it (e.g. e_i to patch (1) and (2)). For brevity, we did not show other patches that cover e_i). Each patch gets a subsequence of the events that it covers, and computes the interim outputs independently (b) with linear attention (f), and the interim outputs of one event are (c) gathered as the final output. In each patch, the embeddings are projected based on their relative position within the patch (e).

different patches. We therefore introduce a position-aware projection (PAP) of the embedding, which projects the embedding based on the event’s relative positions inside the patches.

For an event at \mathbf{x}_i in patch k with top-left global coordinates $\mathbf{c}_k \in \Omega$, we compute its relative position in the patch as

$$\delta_{i,k} = \mathbf{x}_i - \mathbf{c}_k, \quad \text{where } \delta_{i,k} \in \{0, \dots, P-1\}^2. \quad (4)$$

We define the PAP as a linear transform by $\mathbf{W}^{\text{in}} \in \mathbb{R}^{P \times P \times D_{\text{out}} \times D_{\text{in}}}$ and $\mathbf{W}^{\text{out}} \in \mathbb{R}^{P \times P \times D_{\text{out}} \times D_{\text{out}}}$. The input embedding \mathbf{v}_i is projected as

$$\mathbf{u}_{i,k} \in \mathbb{R}^{D_{\text{out}}} \leftarrow \mathbf{W}^{\text{in}}[\delta_{i,k}]\mathbf{v}_i. \quad (5)$$

Then we use $\mathbf{u}_{i,k}$ in patch k as the input of linear attention. Similarly, before aggregating the interim outputs, we also conduct a PAP, and Eq. (3) becomes

$$\mathbf{o}_i = \sum_{k \in \mathcal{K}_i} \mathbf{W}^{\text{out}}[\delta_{i,k}]\mathbf{o}_{i,k}. \quad (6)$$

This projection encodes relative spatial information with learnable parameters, expanding the capability of the model to capture spatial information.

3.3.3. Parallelizable Training

While the MOS structure enables state-level sparsity, it breaks the single state form of linear attention, and thus poses challenges in efficient parallel training on GPUs. To

address this, we derive a *scatter-compute-gather* algorithm, which allows both intra-patch (temporal) and inter-patch (spatial) parallelism to speed up training.

Scatter. Let $\mathbf{u}_{i,k}$ denote the projected embeddings of event e_i for the active patch $k \in \mathcal{K}_i$. We first reorganize the input event sequence \mathcal{E} to K patch-specific subsequences, by constructing a subsequence for each patch k as

$$\mathcal{U}_k = \{\mathbf{u}_{i,k} \mid i \text{ such that } k \in \mathcal{K}_i\}, \quad \forall k \in \mathcal{P}, \quad (7)$$

where \mathcal{U}_k is ordered by t_i . We implement this with a pre-computed lookup table that maps each coordinate in Ω to the indices of the patches covering it, together with its relative position inside each patch. Using the table, we expand \mathcal{E} to a projected sequence \mathcal{U} of length LA , where each event contributes A consecutive projected embeddings, one for each of its activated patches. We apply stable sorting on \mathcal{U} based on the patch indices of each element, forming a reorganized sequence with embeddings in the same patch grouped together as the subsequence, while preserving the temporal order within each \mathcal{U}_k . The resulting permutation is cached and later reused in the gather step.

Compute. All patches share the same parameters but maintain independent states, so that the K subsequences can be computed in parallel, achieving inter-patch parallelism. We apply linear attention (Eq. (1)) to each subse-

Algorithm 1 SSLA Module Training

Require: Events \mathcal{E} , embeddings $\{\mathbf{v}_i\}_{i=1}^L$, coordinates $\{\mathbf{x}_i\}_{i=1}^L$, Patches \mathcal{P} , lookup table $T : \mathbf{x} \in \Omega \mapsto \{(k, \delta)\}$.

Ensure: Updated embeddings $\{\mathbf{o}_i\}_{i=1}^L$ in the same order as the input.

- 1: Initialize an empty embedding sequence \mathcal{U} of length LA .
- 2: **for** each event e_i **in parallel do**
- 3: Lookup \mathbf{x}_i : active patch indices $\{k \mid k \in \mathcal{K}_i\}$, relative positions $\{\delta_{i,k} \mid k \in \mathcal{K}_i\}$;
- 4: Position-aware projection: $\mathbf{u}_{i,k} \leftarrow \mathbf{W}^{\text{in}}[\delta_{i,k}]\mathbf{v}_i$;
- 5: Assign $\mathcal{U}[Ai : A(i+1)] \leftarrow \{\mathbf{u}_{i,k} \mid k \in \mathcal{K}_i\}$
- 6: **end for**
- 7: Scatter \mathcal{U} based on k , and cache the permutation π ;
- 8: Split \mathcal{U} to patch-specific subsequences $\{\mathcal{U}_k \mid k \in \mathcal{P}\}$;
- 9: **for** each patch $k \in \mathcal{P}$ **in parallel do**
- 10: $\mathcal{O}_k \leftarrow \mathbf{LinearAttention}(\mathcal{U}_k)$ using Eq. (1);
- 11: **end for**
- 12: Concat \mathcal{O}_k into interim output sequence \mathcal{O} ;
- 13: Gather: $\mathcal{O} \leftarrow \mathcal{O}[\pi^{-1}]$. We get $\mathcal{O}[Ai : A(i+1)] = \{\mathbf{o}_{i,k} \mid k \in \mathcal{K}_i\}$;
- 14: **for** each event e_i **in parallel do**
- 15: Position-aware projection: $\mathbf{o}_{i,k} \leftarrow \mathbf{W}^{\text{out}}[\delta_{i,k}]\mathbf{o}_{i,k}$;
- 16: **end for**
- 17: Aggregate: $\mathbf{o}_i = \sum \mathcal{O}[Ai : A(i+1)]$;
- 18: **return** $\{\mathbf{o}_i\}_{i=1}^L$

quence \mathcal{U}_k

$$\mathcal{O}_k = \mathbf{LinearAttention}(\mathcal{U}_k), \quad (8)$$

where \mathcal{O}_k contains the interim outputs for events contained in patch k . In each patch, the linear attention is standard, which achieves intra-patch parallelism.

Gather. Finally, we restore the outputs to the original expanded event sequence order using the cached permutation and aggregate the interim outputs from all active patches of each event. Specifically, we first apply the PAP to each interim output $\mathbf{o}_{i,k}$, and then sum them over $k \in \mathcal{K}_i$ according to Eq. (6). This gather step is efficient because it only involves indexed reordering and reduction. The training procedure of the SSLA module is summarized in Algorithm 1.

3.4. Neural Network Details

We propose the SSLA-Det model for asynchronous event-based object detection. An overview of our neural network is shown in Fig. 3, which consists of an asynchronous backbone and a YOLOX detection head [10]. The backbone has 4 stages, each containing 2 SSLA module layers. In the

SSLA layers, we use residual connections [15] and layer normalization [1] to stabilize training. In each stage, we use one sparse pooling and one temporal dropout layer introduced in [36], which compresses event sequence to reduce computation while preserving the high temporal resolution of events. All of the above layers are asynchronous, which makes the backbone fully asynchronous.

SSLA module is agnostic to the specific design of linear attention mechanism, allowing for the integration of any variant, including linear RNNs and SSMs. We use a real-valued Linear Recurrent Unit [27] implemented by Triton [42] in our model for hardware efficiency. The embedding dimension D_{out} has an expansion of $2\times$ in each stage.

For each step, the input to the model is a raw event, with polarity and time difference $\mathbf{v}_i = [p_i, \Delta t_i] \in \mathbb{R}^2$ as the embedding, and the backbone generates \mathbf{o}_i . We form a spatially fine-grained representation $\mathbf{R} \in \mathbb{R}^{H_{out} \times W_{out} \times D_{out}}$ from the asynchronous output, by updating \mathbf{o}_i to $\mathbf{R}[\mathbf{x}_i]$. To realize an end-to-end asynchronicity, we modify the YOLOX head by changing the stem convolution to 1×1 . Each backbone output only updates the head predictions at position \mathbf{x}_i , making the YOLOX head also asynchronous. The whole SSLA-Det model is therefore end-to-end fully asynchronous, leading to minimal latency.

4. Experiments

4.1. Experimental Setup

Datasets. Following previous work [11], we evaluate on the N-Caltech101 Detection [26] and the Gen1 Detection [5] dataset. N-Caltech101 consists of recordings captured by a DAVIS240 event camera with a resolution of 240×180 pixels, undergoing saccadic motion in front of a projector displaying Caltech101 images. Bounding box annotations were manually added in post-processing, with 101 classes. Gen1 is a more challenging, large-scale benchmark for automotive scenarios, recorded by an ATIS event camera with a resolution of 304×240 pixels. The dataset has two categories of 228,123 cars and 27,658 pedestrians. Following previous works [11, 34], we filter out bounding boxes with a diagonal below 30 pixels or width below 20 pixels in Gen1.

Training Details. All experiments were conducted with PyTorch 2.6.0 [30] on NVIDIA Ampere GPUs (A800/RTX 3090). We design four variants of our SSLA-Det model: small (SSLA-S), base (SSLA-B), medium (SSLA-M), and large (SSLA-L), by scaling the embedding dimension D_{out} of the first stage to 12, 16, 24 and 32. We use AdamW [24] optimizer. For Gen1, we train 40 epochs using a batch size of 32 and a base learning rate of 1×10^{-3} with a cosine decay. We use random flipping with probability 0.5 and random dropout of input events with keep ratio $\rho \sim \mathcal{U}(0.8, 1.0)$. For N-Caltech101, we train 200 epochs

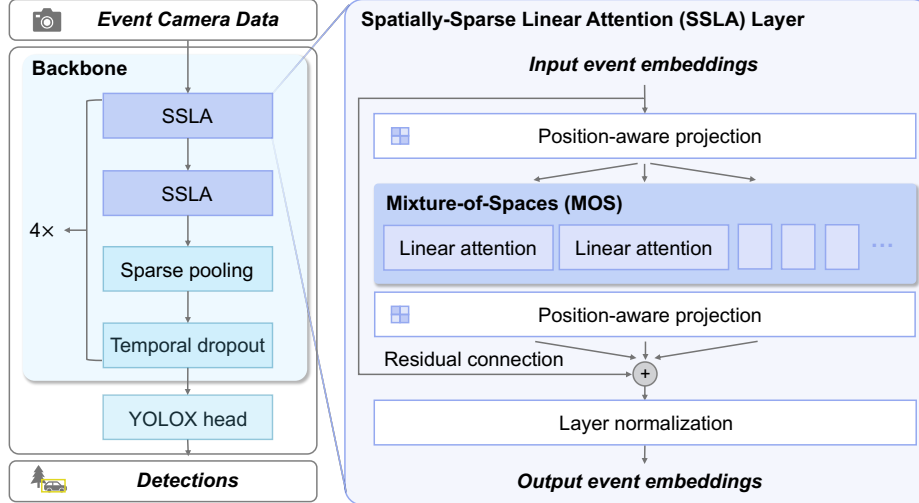


Figure 3. **Overview of the SSLA-Det model.** **Left:** *Fully asynchronous* event-based detector. The input data is processed by a 4-stage asynchronous backbone. Each stage contains 2 SSLA layers followed by sparse pooling and temporal dropout. **Right:** SSLA layer. Input event embeddings are processed by the SSLA module, including two position-aware projections, scatter, parallel patch-wise linear attention and gather. A residual connection and a layer normalization is used for training stability.

with a batch size of 64. In addition to random dropout, we apply random cropping to 75% of the full resolution with probability 0.2 and random translation by up to maximum of 10% of the full resolution following the implementations of [11]. We also use exponential model averaging [17].

4.2. Results

Gen1 Automotive. We compare our SSLA-Det models with asynchronous event-based detection baselines [11, 22, 25, 36, 37], and use synchronous methods as reference [8, 14, 32, 33, 45, 49]. The performance is evaluated in accuracy with mean average precision (mAP) [23] and efficiency with average floating point operations (FLOPS) for every new event. We observed that some prior works report AP_{50} whereas others report mAP, and these values are sometimes presented together in the literature. To avoid potentially misleading comparisons, we separate them in Tab. 1.

Our SSLA-Det models consistently improve the accuracy-efficiency trade-off over existing asynchronous baselines. Notably, compared to the strongest prior asynchronous baseline DAGr-L [11], our smallest model SSLA-S achieves higher mAP (0.334 vs. 0.321) while reducing the computational cost by about $171\times$ (0.102 vs. 17.4 MFLOPS/ev). We attribute this FLOPS advantage mainly to the recurrent architecture and the temporal dropout layer introduced in [36], in which a low FLOPS (0.137 M/ev) was also observed. These components compress the event sequence length at deeper layers, thereby reducing the computation. In contrast, graph-based methods [11, 37] cannot rely on recurrent structures for

temporal accumulation and therefore cannot use the same mechanism to reduce computation. Our largest model, SSLA-L, achieves an mAP of 0.375, setting a new SOTA for asynchronous detection on Gen1, with $> 20\times$ reduction of FLOPS to previous best model DAGr-L (0.724 M/ev vs. 17.4 M/ev).

Fig. 4 visualizes the detection results on Gen1. Fig. 4 (a)-(d) and Fig. 4 (e)-(h) show the detected cars and pedestrians, respectively. Fig. 4 (i)-(l) provide qualitative understandings of the typical failure cases. Specifically, Fig. 4 (i) and (j) show the false negatives, mainly caused by the lack of relative motion between the event camera and the target, which leads to missing event data. Fig. 4 (k) and (l) show the false positives caused by the lack of labels.

N-Caltech101. Tab. 2 presents the performance of our models on the N-Caltech101 dataset. Consistent with the Gen1 results, our models achieve a superior accuracy-efficiency trade-off among asynchronous methods. In particular, SSLA-L reaches an AP_{50} of 0.743 with a computational cost of only 0.926 MFLOPS/ev. Compared with the previous best asynchronous baseline DAGr-L, SSLA-L improves AP_{50} by 1.1 points (0.743 vs. 0.732) while using $20\times$ fewer MFLOPS per event (0.926 vs. 18.9).

4.3. Timing Experiments

Training Efficiency. We show the training efficiency benefit of linear attention with sequential parallelism. We replace linear attention with a long short-term memory (LSTM) baseline [12] with the same hidden dimension as SSLA-S. Tab. 3 compares SSLA with an LSTM baseline

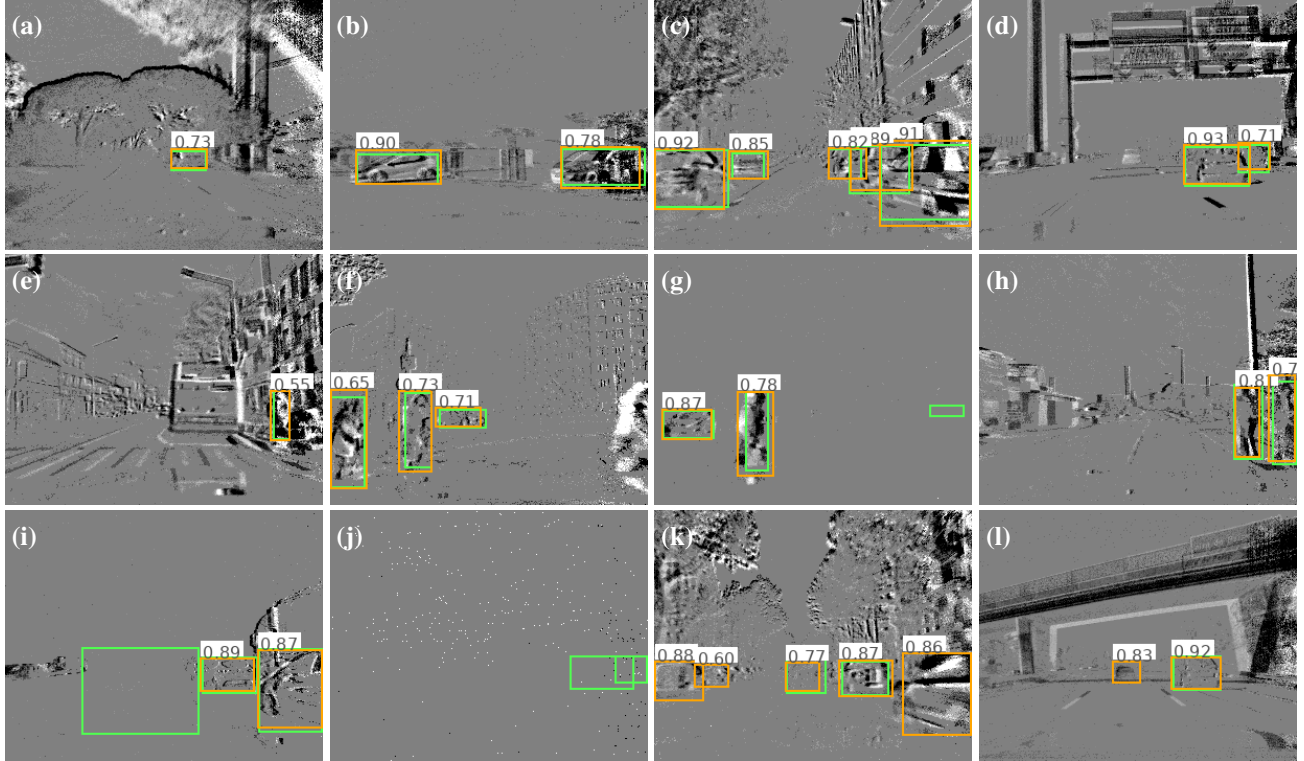


Figure 4. **Visualization of the detection results on the Gen1 dataset.** Green boxes denote ground truth and orange boxes denote predictions with confidence scores. Predicted boxes with confidence scores below 0.5 are removed. (a)-(d): Cars. (e)-(h): Pedestrians. (i)-(l): Failure cases.

from the official PyTorch implementation under the same training setup on Gen1. We compare the training time per epoch, which is measured on 4 NVIDIA A800 GPUs. SSLA-S reduces the epoch time from 1.05 to 0.25 hours ($4.2\times$), but at a cost of a mAP drop (from 0.353 to 0.335), mainly caused by a lower FLOPS. At a similar FLOPS level, SSLA-B achieves comparable mAP to LSTM (0.351 vs. 0.353) and higher AP₅₀ (0.655 vs. 0.631), while reducing training time from 1.05 to 0.28 hours ($3.8\times$).

Inference Latency. We measure the latency of SSLA-Det as the time required to process one newly arrived event in a recurrent, event-by-event setting. We implement a recurrent C++ version of SSLA-Det and benchmark the latency on a single core of an AMD Ryzen 9 9950X3D CPU. As shown in Tab. 4, our models achieve a low latency of less than $10\ \mu\text{s}$, which is lower than the sensor transmission latency of approximately $200\ \mu\text{s}$ [11]. Interestingly, a smaller model does not yield lower latency in our setting (*e.g.* on Gen1, $3.43\ \mu\text{s}$ for SSLA-S and $2.44\ \mu\text{s}$ for SSLA-B), because the actual runtime also depends on hardware factors such as vectorization efficiency and memory access patterns. The SSLA module has a constant per event inference FLOPS of $\mathcal{O}(P^2 D_{out}^2)$, making the latency independent of

resolution. While CPU does not fully translate our FLOPS efficiency into latency gains [11], further runtime latency reduction could be achieved on specific hardware, such as FPGAs [18] or neuromorphic accelerators [48].

4.4. Ablation Study

Effect of Spatial-Sparsity. We replace the SSLA module with a standard linear attention (LRU). We use D_{out} of the first stage 12 and 36, to keep same D_{out} and similar FLOPS as SSLA-S. Tab. 5 shows that using a standard linear attention fails in both cases, which is considered mainly due to the lack of fine-grained state. In particular, SSLA-S maintains a state $380\times$ larger than LA ($D_{out} = 36$) with similar FLOPS (0.102 M/ev vs. 0.093 M/ev). This demonstrates the importance of state-level sparsity.

Effect of Position-Aware Projection. To ablate PAP, we replace it with a position-irrelevant learnable linear projection. The results are summarized in Tab. 6. Removing either input or output PAP causes a significant accuracy drop, and removing both results in catastrophic failure, with the mAP collapsing to only 0.014, which highlights its importance for encoding spatial priors and introducing translation invariance in SSLA module.

Table 1. **Object detection results on the Gen1 Detection dataset.** Async. refers to asynchronous methods.

Method	Async.	mAP(\uparrow)	AP ₅₀ (\uparrow)	MFLOPS/ev(\downarrow)
EVA+RVT-B [14]	✗	0.477	-	3.5×10^3
GET [32]	✗	0.479	-	3.6×10^3
SAST-CB [33]	✗	0.482	-	2.4×10^3
SMamba [45]	✗	0.504	-	2.4×10^3
ERGO-12 [49]	✗	0.504	-	50.8×10^3
EventPillars [8]	✗	0.531	-	50.8×10^3
NVS-S [22]	✓	-	0.086	7.80
AsyNet [25]	✓	-	0.145	205
AEGNN [37]	✓	-	0.163	5.26
FARSE-CNN [36]	✓	-	0.300	0.137
DAGr-N [11]	✓	0.263	-	1.36
DAGr-S [11]	✓	0.304	-	4.58
DAGr-M [11]	✓	0.318	-	9.94
DAGr-L [11]	✓	0.321	-	17.4
SSLA-S (Ours)	✓	0.334	0.629	0.102
SSLA-B (Ours)	✓	0.351	0.655	0.182
SSLA-M (Ours)	✓	0.370	0.670	0.408
SSLA-L (Ours)	✓	0.375	0.675	0.724

Table 2. **Object detection results on the N-Caltech101 Detection dataset.** Async. refers to asynchronous methods.

Method	Async.	mAP(\uparrow)	AP ₅₀ (\uparrow)	MFLOPS/ev(\downarrow)
NVS-S [22]	✓	-	0.346	7.80
AsyNet [25]	✓	-	0.643	200
AEGNN [37]	✓	-	0.595	7.41
EHGCN [2]	✓	-	0.694	1.06
DAGr-N [11]	✓	-	0.629	2.28
DAGr-S [11]	✓	-	0.702	6.85
DAGr-M [11]	✓	-	0.727	12.2
DAGr-L [11]	✓	-	0.732	18.9
SSLA-S (Ours)	✓	0.444	0.681	0.131
SSLA-B (Ours)	✓	0.483	0.720	0.233
SSLA-M (Ours)	✓	0.495	0.724	0.522
SSLA-L (Ours)	✓	0.515	0.743	0.926

Table 3. **Comparison of training efficiency between SSLA and an LSTM baseline on Gen1.** Time refers to the training time per epoch measured on 4 NVIDIA A800 GPUs.

Method	Time (h)(\downarrow)	mAP(\uparrow)	AP ₅₀ (\uparrow)	Params	MFLOPS/ev(\downarrow)
SSLA-S	0.25	0.335	0.629	0.508 M	0.102
SSLA-B	0.28	0.351	0.655	0.868 M	0.182
LSTM	1.05	0.353	0.631	0.606 M	0.176

Effect of Patch Size. P controls the receptive field of event interaction. As shown in Tab. 7, a smaller patch size ($P = 2$) reduces FLOPS (0.047 M/ev) but leads to a mAP drop (0.200). Conversely, $P = 4$ boosts the mAP

Table 4. **Inference latency.** Latency refers to the time used for the recurrent model to process a new event.

Dataset	Resolution	Latency (μ s)			
		SSLA-S	SSLA-B	SSLA-M	SSLA-L
Gen1	304×240	3.43	2.44	6.02	7.20
N-Caltech101	240×180	3.60	2.61	6.50	8.01

Table 5. **Effect of Spatial-Sparsity.** We use linear attention (LA) with same embedding dimension (first stage $D_{out} = 12$) and similar FLOPS (first stage $D_{out} = 36$) compared to SSLA-S. We report accuracy on the validation set of Gen1. State refers to the size of hidden state in the last layer, which reflects the capability to model fine-grained spatial representations.

Model	mAP	AP ₅₀	AP ₇₅	MFLOPS/ev	Params	State
SSLA-S	0.355	0.610	0.322	0.102	0.508 M	106.9 K
LA (12)	0.001	0.004	0.000	0.011	0.130 M	0.094 K
LA (36)	0.001	0.003	0.000	0.093	1.20 M	0.281 K

Table 6. **Effect of Position-Aware Projection.** Input and Output refer to the PAP with \mathbf{W}^{in} and \mathbf{W}^{out} , respectively. We report accuracy on the validation set of Gen1.

PAP		mAP(\uparrow)	AP ₅₀ (\uparrow)	AP ₇₅ (\uparrow)	MFLOPS/ev(\downarrow)
Input	Output				
✓	✓	0.335	0.610	0.322	0.102
✓		0.306	0.582	0.280	0.085
	✓	0.224	0.473	0.184	0.089
		0.014	0.048	0.006	0.072

Table 7. **Effect of Patch Size.** We report accuracy on the validation set of Gen1.

Patch Size	mAP(\uparrow)	AP ₅₀ (\uparrow)	AP ₇₅ (\uparrow)	MFLOPS/ev(\downarrow)
$P = 2$	0.200	0.440	0.150	0.047
$P = 3$	0.335	0.610	0.322	0.102
$P = 4$	0.371	0.656	0.364	0.179

to 0.371 but increases the FLOPS to 0.179 M/ev, showing an accuracy-efficiency trade-off. Besides, for training, increasing P results in higher GPU memory consumption and longer training time. Therefore, we select $P = 3$ as our default configuration as it yields a reasonable trade-off between efficiency and accuracy.

5. Limitation and Discussion

This work focuses on event-based low-latency object detection. While hybrid event-image models become a recent research trend [11, 21], they also introduce additional challenges, including event-image alignment, extra sensor re-

quirements, and high system complexity. Besides, in principle, our method is also compatible with the hybrid framework, since image features from dense models can be injected into the intermediate layers of our model. Exploring this event-image fusion in SSLA is an interesting direction for our future work.

Although SSLA-Det achieves SOTA performance among asynchronous event-based detectors, it still lags behind synchronous methods (*e.g.*, on Gen1, 0.375 mAP for SSLA-L while >0.5 mAP for synchronous SOTA [8]). Scaling the model may potentially narrow this gap, but long event sequences make GPU memory consumption a key bottleneck. Due to hardware limitations, we have not yet studied large-scale variants of our SSLA models, and we leave a thorough scaling analysis to future work.

Finally, we observe an interesting architectural resemblance between SSLA and recurrent submanifold models, like FARSE-CNN [36]. In particular, PAP introduces a translation invariance inductive bias, similar to the role of convolution in FARSE-CNN [36], suggesting some key designs for asynchronous event processing. However, SSLA and FARSE-CNN [36] differ in information aggregation manners. SSLA explicitly gathers information from multiple patches and aggregates them to preserve sparsity, rather than keeping only the output in the submanifold to preserve sparsity, enabling better spatial integration and contributing to accuracy improvements.

6. Conclusion

In this paper, we propose SSLA, a novel linear attention module with spatial sparsity and efficient parallel training capability for event sequence modeling. We develop SSLA-Det, the first end-to-end asynchronous linear attention-based model for event-based object detection. Experimental results on Gen1 and N-Caltech101 show that SSLA-Det achieves SOTA asynchronous accuracy with significantly lower FLOPS than previous asynchronous baselines. We believe that SSLA provides a promising direction for low-latency, high-performance event-based perception.

References

- [1] Jimmy Lei Ba, Jamie Ryan Kiros, and Geoffrey E Hinton. Layer normalization. *arXiv preprint arXiv:1607.06450*, 2016. 5
- [2] Haosheng Chen, Lian Luo, Mengjingcheng Mo, Zhanjie Wu, Guobao Xiao, Ji Gan, Jiayu Leng, and Xinbo Gao. EhgcN: Hierarchical euclidean-hyperbolic fusion via motion-aware gcN for hybrid event stream perception. *arXiv preprint arXiv:2504.16616*, 2025. 2, 8
- [3] Thomas Dalgaty, Thomas Mesquida, Damien Joubert, Amos Sironi, Pascal Vivet, and Christoph Posch. Hugnet: Hemispherical update graph neural network applied to low-latency event-based optical flow. In *Proceedings of the IEEE/CVF Conference on Computer Vision and Pattern Recognition*, pages 3953–3962, 2023. 2
- [4] Manon Dampffoffer, Thomas Mesquida, Damien Joubert, Thomas Dalgaty, Pascal Vivet, and Christoph Posch. Graph neural network combining event stream and periodic aggregation for low-latency event-based vision. In *Proceedings of the IEEE/CVF Conference on Computer Vision and Pattern Recognition*, pages 6909–6918, 2025. 2
- [5] Pierre De Tournemire, Davide Nitti, Etienne Perot, Davide Migliore, and Amos Sironi. A large scale event-based detection dataset for automotive. *arXiv preprint arXiv:2001.08499*, 2020. 5
- [6] Jusen Du, Weigao Sun, Disen Lan, Jiayi Hu, Tao Zhang, and Yu Cheng. Mom: Linear sequence modeling with mixture-of-memories. In *The Fourteenth International Conference on Learning Representations*, 2026. 2, 3
- [7] Davide Falanga, Kevin Kleber, and Davide Scaramuzza. Dynamic obstacle avoidance for quadrotors with event cameras. *Science Robotics*, 5(40):eaaz9712, 2020. 1
- [8] Rui Fan, Weidong Hao, Juntao Guan, Lai Rui, Lin Gu, Tong Wu, Fanhong Zeng, and Zhangming Zhu. Eventpillars: Pillar-based efficient representations for event data. In *Proceedings of the AAAI Conference on Artificial Intelligence*, pages 2861–2869, 2025. 6, 8, 9
- [9] Guillermo Gallego, Tobi Delbrück, Garrick Orchard, Chiara Bartolozzi, Brian Taba, Andrea Censi, Stefan Leutenegger, Andrew J Davison, Jörg Conradt, Kostas Daniilidis, et al. Event-based vision: A survey. *IEEE transactions on pattern analysis and machine intelligence*, 44(1):154–180, 2020. 1, 2
- [10] Zheng Ge, Songtao Liu, Feng Wang, Zeming Li, and Jian Sun. Yolox: Exceeding yolo series in 2021. *arXiv preprint arXiv:2107.08430*, 2021. 5
- [11] Daniel Gehrig and Davide Scaramuzza. Low-latency automotive vision with event cameras. *Nature*, 629(8014):1034–1040, 2024. 1, 2, 5, 6, 7, 8
- [12] Alex Graves. Long short-term memory. *Supervised sequence labelling with recurrent neural networks*, pages 37–45, 2012. 6
- [13] Albert Gu and Tri Dao. Mamba: Linear-time sequence modeling with selective state spaces. In *First conference on language modeling*, 2024. 1, 3
- [14] Haiqing Hao, Nikola Zubic, Weihua He, Zhipeng Sui, Davide Scaramuzza, and Wenhui Wang. Maximizing asynchronicity in event-based neural networks. In *The Fourteenth International Conference on Learning Representations*, 2026. 1, 2, 3, 6, 8
- [15] Kaiming He, Xiangyu Zhang, Shaoqing Ren, and Jian Sun. Deep residual learning for image recognition. In *Proceedings of the IEEE conference on computer vision and pattern recognition*, pages 770–778, 2016. 5
- [16] Weihua He, Junwen Zhu, Yongxiang Feng, Fei Liang, Kaichao You, Huichao Chai, Zhipeng Sui, Haiqing Hao, Guoqi Li, Jingjing Zhao, et al. Neuromorphic-enabled video-activated cell sorting. *Nature communications*, 15(1):10792, 2024. 1
- [17] Pavel Izmailov, Dmitrii Podoprikin, Timur Garipov, Dmitry Vetrov, and Andrew Gordon Wilson. Averaging weights

- leads to wider optima and better generalization. *arXiv preprint arXiv:1803.05407*, 2018. 6
- [18] Kamil Jeziorek, Piotr Wzorek, Krzysztof Blachut, Hiroshi Nakano, Manon Dampfhofer, Thomas Mesquida, Hiroaki Nishi, Thomas Dalgaty, and Tomasz Kryjak. Hardware-accelerated graph neural networks: an alternative approach for neuromorphic event-based audio classification and keyword spotting on soc fpga. *arXiv preprint arXiv:2602.16442*, 2026. 7
- [19] Uday Kamal, Saurabh Dash, and Saibal Mukhopadhyay. Associative memory augmented asynchronous spatiotemporal representation learning for event-based perception. In *The Eleventh International Conference on Learning Representations*, 2023. 2, 3
- [20] Angelos Katharopoulos, Apoorv Vyas, Nikolaos Pappas, and François Fleuret. Transformers are rnns: Fast autoregressive transformers with linear attention. In *International conference on machine learning*, pages 5156–5165. PMLR, 2020. 1, 3
- [21] Dianze Li, Jianing Li, Xu Liu, Xiaopeng Fan, and Yonghong Tian. Asynchronous collaborative graph representation for frames and events. In *Proceedings of the Computer Vision and Pattern Recognition Conference*, pages 1655–1666, 2025. 8
- [22] Yijin Li, Han Zhou, Bangbang Yang, Ye Zhang, Zhaopeng Cui, Hujun Bao, and Guofeng Zhang. Graph-based asynchronous event processing for rapid object recognition. In *Proceedings of the IEEE/CVF International Conference on Computer Vision*, pages 934–943, 2021. 2, 6, 8
- [23] Tsung-Yi Lin, Michael Maire, Serge Belongie, James Hays, Pietro Perona, Deva Ramanan, Piotr Dollár, and C Lawrence Zitnick. Microsoft coco: Common objects in context. In *European conference on computer vision*, pages 740–755. Springer, 2014. 6
- [24] Ilya Loshchilov and Frank Hutter. Decoupled weight decay regularization. In *International Conference on Learning Representations*, 2019. 5
- [25] Nico Messikommer, Daniel Gehrig, Antonio Loquercio, and Davide Scaramuzza. Event-based asynchronous sparse convolutional networks. In *European Conference on Computer Vision*, pages 415–431. Springer, 2020. 2, 6, 8
- [26] Garrick Orchard, Ajinkya Jayawant, Gregory K Cohen, and Nitish Thakor. Converting static image datasets to spiking neuromorphic datasets using saccades. *Frontiers in neuroscience*, 9:437, 2015. 5
- [27] Antonio Orvieto, Samuel L Smith, Albert Gu, Anushan Fernando, Caglar Gulcehre, Razvan Pascanu, and Soham De. Resurrecting recurrent neural networks for long sequences. In *International conference on machine learning*, pages 26670–26698. PMLR, 2023. 5
- [28] Yuqi Pan, Yongqi An, Zheng Li, Yuhong Chou, Rui-Jie Zhu, Xiaohui Wang, Mingxuan Wang, Jinqiao Wang, and Guoqi Li. Scaling linear attention with sparse state expansion. In *The Fourteenth International Conference on Learning Representations*, 2026. 3
- [29] Federico Paredes-Vallés, Jesse J Hagensaaers, Julien Dupeyroux, Stein Stroobants, Yingfu Xu, and Guido CHE de Croon. Fully neuromorphic vision and control for autonomous drone flight. *Science Robotics*, 9(90):eadi0591, 2024. 1
- [30] Adam Paszke, Sam Gross, Francisco Massa, Adam Lerer, James Bradbury, Gregory Chanan, Trevor Killeen, Zeming Lin, Natalia Gimelshein, Luca Antiga, et al. Pytorch: An imperative style, high-performance deep learning library. *Advances in neural information processing systems*, 32, 2019. 5
- [31] Bo Peng, Eric Alcaide, Quentin Anthony, Alon Albalak, Samuel Arcadinho, Stella Biderman, Huanqi Cao, Xin Cheng, Michael Chung, Leon Derczynski, et al. Rvkv: Reinventing rnns for the transformer era. In *Findings of the association for computational linguistics: EMNLP 2023*, pages 14048–14077, 2023. 1
- [32] Yansong Peng, Yueyi Zhang, Zhiwei Xiong, Xiaoyan Sun, and Feng Wu. Get: Group event transformer for event-based vision. In *Proceedings of the IEEE/CVF International Conference on Computer Vision*, pages 6038–6048, 2023. 1, 6, 8
- [33] Yansong Peng, Hebei Li, Yueyi Zhang, Xiaoyan Sun, and Feng Wu. Scene adaptive sparse transformer for event-based object detection. In *Proceedings of the IEEE/CVF conference on computer vision and pattern recognition*, pages 16794–16804, 2024. 6, 8
- [34] Etienne Perot, Pierre De Tournemire, Davide Nitti, Jonathan Masci, and Amos Sironi. Learning to detect objects with a 1 megapixel event camera. *Advances in Neural Information Processing Systems*, 33:16639–16652, 2020. 5
- [35] Charles R Qi, Hao Su, Kaichun Mo, and Leonidas J Guibas. Pointnet: Deep learning on point sets for 3d classification and segmentation. In *Proceedings of the IEEE conference on computer vision and pattern recognition*, pages 652–660, 2017. 2
- [36] Riccardo Santambrogio, Marco Cannici, and Matteo Matteucci. Farse-cnn: Fully asynchronous, recurrent and sparse event-based cnn. In *European conference on computer vision*, pages 1–18. Springer, 2024. 1, 2, 5, 6, 8, 9
- [37] Simon Schaefer, Daniel Gehrig, and Davide Scaramuzza. Aegnn: Asynchronous event-based graph neural networks. In *Proceedings of the IEEE/CVF conference on computer vision and pattern recognition*, pages 12371–12381, 2022. 1, 2, 6, 8
- [38] Mark Schöne, Neeraj Mohan Sushma, Jingyue Zhuge, Christian Mayr, Anand Subramoney, and David Kappel. Scalable event-by-event processing of neuromorphic sensory signals with deep state-space models. In *2024 International Conference on Neuromorphic Systems (ICONS)*, pages 124–131. IEEE, 2024. 1, 2, 3
- [39] Yusuke Sekikawa, Kosuke Hara, and Hideo Saito. Eventnet: Asynchronous recursive event processing. In *Proceedings of the IEEE/CVF conference on computer vision and pattern recognition*, pages 3887–3896, 2019. 1, 2
- [40] Yusuke Sekikawa, Jun Nagata, Itsumi Araki, and Andreu Girbau. Col2a: Convolution-free local linear attention for spatiotemporal event processing. In *Proceedings of the IEEE/CVF Winter Conference on Applications of Computer Vision*, pages 4869–4880, 2026. 3

- [41] Taylan Soydan, Nikola Zubić, Nico Messikommer, Siddhartha Mishra, and Davide Scaramuzza. S7: Selective and simplified state space layers for sequence modeling. *arXiv preprint arXiv:2410.03464*, 2024. 1, 2, 3
- [42] Philippe Tillet, Hsiang-Tsung Kung, and David Cox. Triton: an intermediate language and compiler for tiled neural network computations. In *Proceedings of the 3rd ACM SIGPLAN International Workshop on Machine Learning and Programming Languages*, pages 10–19, 2019. 5
- [43] Carmen Martin Turrero, Maxence Bouvier, Manuel Breitenstein, Pietro Zanuttigh, and Vincent Parret. ALERT-transformer: Bridging asynchronous and synchronous machine learning for real-time event-based spatio-temporal data. In *Forty-first International Conference on Machine Learning*, 2024. 2
- [44] Ashish Vaswani, Noam Shazeer, Niki Parmar, Jakob Uszkoreit, Llion Jones, Aidan N Gomez, Łukasz Kaiser, and Illia Polosukhin. Attention is all you need. *Advances in neural information processing systems*, 30, 2017. 3
- [45] Nan Yang, Yang Wang, Zhanwen Liu, Meng Li, Yisheng An, and Xiangmo Zhao. Smamba: Sparse mamba for event-based object detection. In *Proceedings of the AAAI Conference on Artificial Intelligence*, pages 9229–9237, 2025. 6, 8
- [46] Songlin Yang, Bailin Wang, Yikang Shen, Rameswar Panda, and Yoon Kim. Gated linear attention transformers with hardware-efficient training. *arXiv preprint arXiv:2312.06635*, 2023. 1, 3
- [47] Songlin Yang, Bailin Wang, Yu Zhang, Yikang Shen, and Yoon Kim. Parallelizing linear transformers with the delta rule over sequence length. *Advances in neural information processing systems*, 37:115491–115522, 2024. 1
- [48] Xiaoyu Zhang, Mingtao Hu, Sen Lu, Soohyeon Kim, Eric Yeu-Jer Lee, Yuyang Liu, and Wei D Lu. Compute-in-memory implementation of state space models for event sequence processing. *Nature Communications*, 2026. 7
- [49] Nikola Zubić, Daniel Gehrig, Mathias Gehrig, and Davide Scaramuzza. From chaos comes order: Ordering event representations for object recognition and detection. In *Proceedings of the IEEE/CVF International Conference on Computer Vision*, pages 12846–12856, 2023. 1, 6, 8